



ELSEVIER

# FEBS Letters

journal homepage: [www.FEBSLetters.org](http://www.FEBSLetters.org)

## SAP97 promotes the stability of Na<sub>x</sub> channels at the plasma membrane

Q1 Masahito Matsumoto<sup>a</sup>, Akihiro Fujikawa<sup>a</sup>, Ryoko Suzuki<sup>a</sup>, Hidetada Shimizu<sup>a</sup>, Kazuya Kuboyama<sup>a</sup>,  
Takeshi Y. Hiyama<sup>a,b</sup>, Randy A. Hall<sup>c</sup>, Masaharu Noda<sup>a,b,\*</sup>

<sup>a</sup> Division of Molecular Neurobiology, National Institute for Basic Biology, 5-1 Higashiyama, Myodaiji-cho, Okazaki, Aichi 444-8787, Japan

<sup>b</sup> School of Life Science, The Graduate University for Advanced Studies, 5-1 Higashiyama, Myodaiji-cho, Okazaki, Aichi 444-8787, Japan

<sup>c</sup> Department of Pharmacology, Rollins Research Center, Emory University School of Medicine, Atlanta, GA 30322, USA

### ARTICLE INFO

#### Article history:

Received 2 August 2012

Revised 30 August 2012

Accepted 10 September 2012

Available online xxx

Edited by Maurice Montal

#### Keywords:

Sodium channel

PDZ array

PDZ-binding motif

MAGUK protein

Subfornical organ

Astrocyte

### ABSTRACT

**Na<sub>x</sub> is a sodium-level sensor for body fluids expressed in the circumventricular organs in the brain. Na<sub>x</sub> has a putative PSD95/Disc-large/ZO1 (PDZ)-binding motif at the carboxyl (C)-terminus. Here we found that several PDZ proteins bind to Na<sub>x</sub> by PDZ-array overlay assay. Among them, synapse-associated protein 97 (SAP97/DLG1) was coexpressed with Na<sub>x</sub> in the subfornical organ. In C6 glioblastoma cells, destruction of the PDZ-binding motif of Na<sub>x</sub> or depletion of SAP97 resulted in a decrease in cell-surface Na<sub>x</sub>, which was attenuated with inhibitors of endocytosis. These results indicate that SAP97 contributes to the stabilization of Na<sub>x</sub> channels at the plasma membrane.**

#### Structured summary of protein interactions:

**Na<sub>x</sub>** physically interacts with **SAP97** by anti tag coimmunoprecipitation (View interaction)

**CNRasGEF** binds to **Na<sub>x</sub>** by protein array (View interaction)

**Na<sub>x</sub>** and **SAP97** colocalize by fluorescence microscopy (View interaction)

**GIPC1** binds to **Na<sub>x</sub>** by protein array (View interaction)

**ZO-1** binds to **Na<sub>x</sub>** by protein array (View interaction)

**SAP97** binds to **Na<sub>x</sub>** by protein array (View interaction)

**Densin-180** binds to **Na<sub>x</sub>** by protein array (View interaction)

**Beta-1-syntrophin** binds to **Na<sub>x</sub>** by protein array (View interaction)

**ERBIN** binds to **Na<sub>x</sub>** by protein array (View interaction)

**Na<sub>x</sub>** physically interacts with **SAP97** by pull down (View interaction)

**Ln<sub>x</sub>1** binds to **Na<sub>x</sub>** by protein array (View interaction)

**nNOS** binds to **Na<sub>x</sub>** by protein array (View interaction)

© 2012 Published by Elsevier B.V. on behalf of the Federation of European Biochemical Societies.

### 1. Introduction

Sodium (Na) is a major electrolyte of extracellular fluids and the main determinant of osmolality. Na homeostasis is essential to life and Na<sup>+</sup> concentrations in plasma and cerebrospinal fluid (CSF) are continuously monitored to maintain a physiological level of Na<sup>+</sup> in body fluids [1]. We have previously shown that Na<sub>x</sub>, which structurally resembles voltage-gated sodium channels (Na<sub>v</sub>1.1–1.9), is a concentration-sensitive Na channel with a threshold of ~150 mM for extracellular Na<sup>+</sup> concentration [Na<sup>+</sup>]<sub>o</sub> in vitro [2–4].

In the brain, Na<sub>x</sub> channels are specifically expressed in astrocytes and ependymal cells in the sensory circumventricular organs (sCVOs), such as the subfornical organ (SFO) and organum vasculosum of the lamina terminalis (OVLT), where Na<sub>x</sub>-positive glial cells are involved in sensing an increase in [Na<sup>+</sup>] in body fluids [5]. Na<sub>x</sub>-Deficient mice do not stop ingesting salt even when dehydrated, while wild-type mice avoid salt [6]. This behavioral defect of Na<sub>x</sub>-deficient mice is recovered by a site-directed transfer of the Na<sub>x</sub> gene with an adenoviral vector into the SFO [7]. Na<sub>x</sub> thus functions as the brain's Na<sup>+</sup>-level sensor for the homeostatic control of [Na<sup>+</sup>] in body fluids.

Some PDZ domain-containing proteins are known to serve as key scaffolds for channel proteins to control their trafficking [8]. PDZ domains are 90 amino-acid protein–protein interaction modules that bind to specific C-terminal motifs in their target proteins [9]. Most of the target proteins have a conserved PDZ-binding

\* Corresponding author at: Division of Molecular Neurobiology, National Institute for Basic Biology, 5-1 Higashiyama, Myodaiji-cho, Okazaki, Aichi 444-8787, Japan. Fax: +81 564 59 5845.

E-mail address: [madon@nibb.ac.jp](mailto:madon@nibb.ac.jp) (M. Noda).

78 motif that matches one of the three 'canonical' consensus motifs  
 79 (Class I,  $-X-S/T-X-L/V$ ; Class II,  $-X-\Psi-X-\Psi$ ; Class III,  $-X-D/E-$   
 80  $X-L/V$ ;  $\Psi$  indicates hydrophobic amino acid; [9]). Giallourakis  
 81 et al. [9] recently found a new consensus motif ( $-X-S/T-X-I/A$ )  
 82 other than the 'canonical' motifs. Because the C-terminal sequence  
 83 of  $Na_x$  ( $-Q-T-Q-I$  for rat and mouse, and  $-Q-S-Q-I$  for human) fits  
 84 this 'non-canonical' PDZ-binding motif, we hypothesized that the  
 85  $Na_x$  channel may be regulated by PDZ-scaffold proteins. In the  
 86 present study, we took advantage of a proteomic PDZ-domain array  
 87 [10], containing 96 distinct PDZ domains, to screen for PDZ pro-  
 88 teins that might interact with  $Na_x$ . Among the PDZ proteins thus  
 89 identified, we found that SAP97 (also known as DLG1) is coex-  
 90 pressed with  $Na_x$  in the SFO, and contributes to the stability of  $Na_x$   
 91 channels in the plasma membrane.

## 92 2. Materials and methods

### 93 2.1. Recombinant proteins

94 The Glutathione S-transferase (GST)-fused protein with the C-  
 95 terminal region (amino acid residues 1489–1681) of mouse  $Na_x$   
 96 (GST- $Na_x$ -C-term), its PDZ-binding-motif mutant (GST- $Na_x$ -C-  
 97 term-T1679A) in which Thr-1679 was replaced with Ala, or its  
 98 PDZ-binding-motif deletion mutant (GST- $Na_x$ -C-term $\Delta$ TQI) was  
 99 expressed in an *Escherichia coli* strain, BL21, and purified by gluta-  
 100 thione affinity chromatography as described [11].

### 101 2.2. Overlay assay on the PDZ array

102 The PDZ-array overlay assay was performed as described  
 103 [10,12]. Briefly, a nylon membrane spotted with a series of His/  
 104 S-tagged PDZ domain proteins was pre-treated with a blocking  
 105 buffer containing 2% non-fat dry milk and 0.1% Tween-20 in  
 106 150 mM NaCl and 10 mM phosphate buffer, pH 7.3 (PBS) for  
 107 30 min, then overlaid with the GST-fused proteins (15 nM) in the

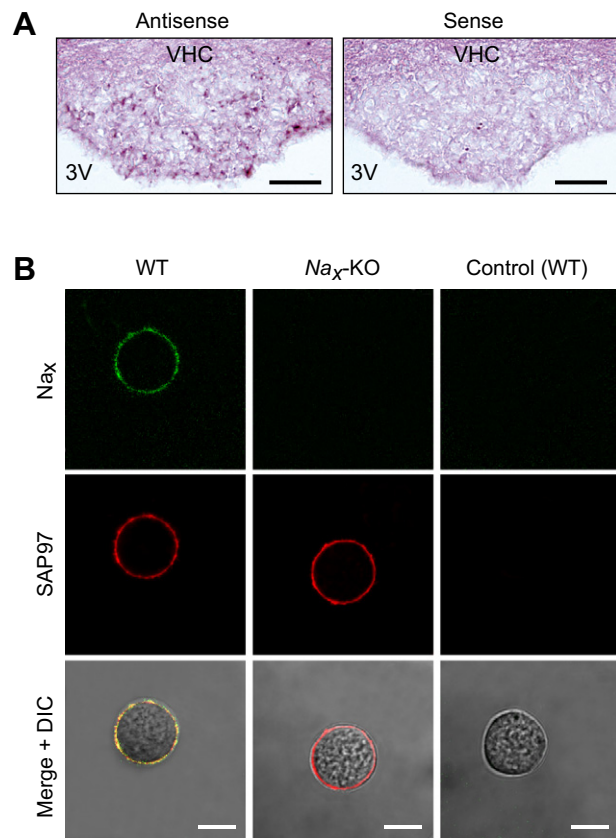


**Fig. 2.** Expression of  $Na_x$  and SAP97. (A) Expression of SAP97 in the SFO. Coronal tissue sections of the mouse SFO were hybridized with antisense SAP97, or with the control sense probe. VHC, ventral hippocampal commissure; 3V, dorsal third ventricle. Scale bars, 50  $\mu$ m. (B) Double immunostaining of SFO cells obtained from wild type (WT; left) and  $Na_x$ -knockout ( $Na_x$ -KO; middle) mice with anti- $Na_x$  and anti-SAP97 antibodies. Right panels show the results of control experiments omitting the primary antibodies. Scale bars, 10  $\mu$ m.

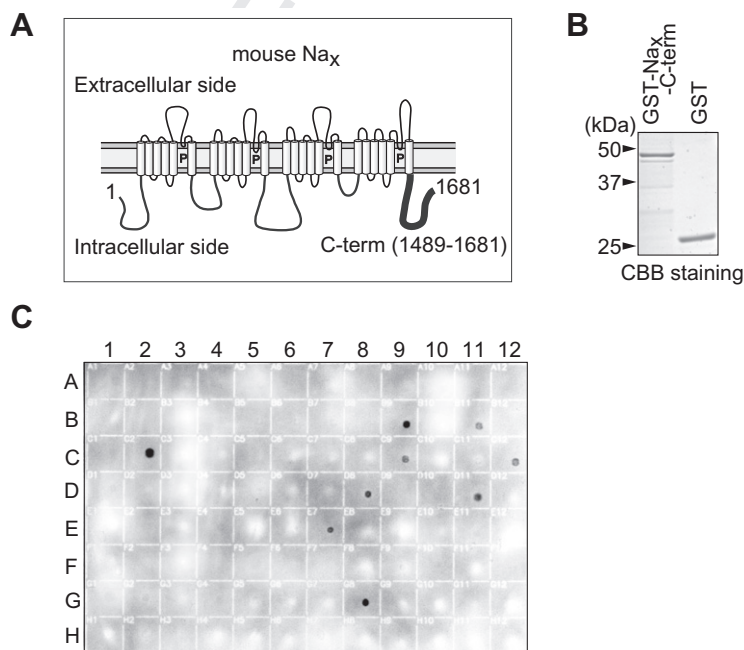


**Fig. 1.** Screening of PDZ proteins that bind to the C-terminus of  $Na_x$ . (A) Schematic drawing of  $Na_x$ . The C-terminal region of  $Na_x$  used for preparation of the recombinant GST-fused protein (GST- $Na_x$ -C-term) is indicated with a bold line. (B) Preparation of GST- $Na_x$ -C-term and control GST proteins. The purity was checked by Coomassie Brilliant Blue R-250 (CBB) staining following SDS-PAGE. (C) PDZ array overlay assay with GST- $Na_x$ -C-term. For the proteins spotted on the array, see Supplementary Information (Table S1). Strong positive hits were observed for CNRasGEF-PDZ (B9), SAP97-PDZ1+2 (C2), and LNX1-PDZ3 (G8).

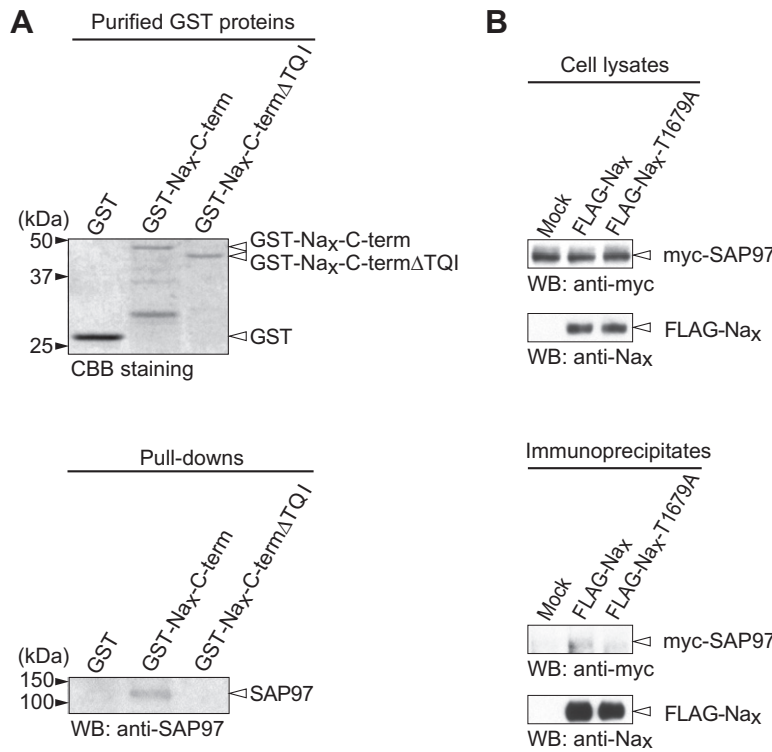


**Fig. 3.** Binding of SAP97 with Na<sub>x</sub>. (A) In vitro binding assay of SAP97 and the C-terminal region of the Na<sub>x</sub> channel. Input proteins were visualized by CBB staining (upper). Glutathione beads coated with GST, GST-Na<sub>x</sub>-C-term, or GST-Na<sub>x</sub>-C-termΔTQI (PDZ-binding-motif deletion mutant) were incubated with the lysate of C6 cells. The bound endogenous SAP97 was detected by Western blotting with anti-SAP97 (lower). (B) Binding of the full-length Na<sub>x</sub> to SAP97 in HEK293T cells. The expression construct for myc-tagged SAP97 was transfected into HEK293T cells, together with the control vector, FLAG-tagged wild-type Na<sub>x</sub>, or its FLAG-tagged PDZ-binding-motif mutant. The amounts of protein expressed in the cell extract (upper two panels), and immunoprecipitated with anti-FLAG M2 (lower two panels), were analyzed by Western blotting using anti-myc (for detection of SAP97) and anti-Na<sub>x</sub>.

108 blocking buffer. The binding was detected with a horseradish  
109 peroxidase-conjugated anti-GST antibody (GE Healthcare), and  
110 visualized by enhanced chemiluminescence (GE Healthcare).

111 **2.3. In situ hybridization**

112 In situ hybridization was performed as described [13] on coronal  
113 brain sections of C57BL/6 mice (male, 4 months old) by using  
114 cRNA probes synthesized from pGEM T-Easy vector (Promega)  
115 carrying the 812-base fragment of mouse SAP97 (nucleotides  
116 694–1506, GenBank accession number NM\_007862).

117 **2.4. Dissociation of the SFO cells**

118 The SFO was dissected from fresh brain slices of Na<sub>x</sub>-knockout  
119 [6] or control C57BL/6 mice (male, 2 months old), and SFO cells  
120 were dissociated as described [2]. Isolated cells were attached on  
121 glass-bottomed dishes coated with Cell-tak (BD Biosciences) in  
122 DMEM containing 10% fetal calf serum (FCS) in a humidity-controlled  
123 incubator gassed with 5% CO<sub>2</sub> for 3 h at 37 °C.

124 **2.5. Immunofluorescence cell staining**

125 SFO cells and rat C6 cells were fixed with 4% paraformaldehyde  
126 in PBS, and microwaved in 10 mM citrate buffer, pH 6.0. After  
127 blocking with 4% non-fat dry milk and 0.1% Tween 20 in PBS, the  
128 cells were incubated with rabbit anti-Na<sub>x</sub> [2] and mouse anti-  
129 SAP97 (Cat. No. 610874; BD Biosciences) in the blocking buffer  
130 for 1 week at 4 °C. Bound antibodies were visualized with

Alexa488-conjugated anti-rabbit and Alexa594-conjugated anti-  
131 mouse antibodies (Life Technologies), respectively. 132

133 **2.6. Expression plasmid construction and DNA transfection to**  
134 **HEK293T cells**

135 The expression construct of the PDZ-binding motif mutant  
136 (pTRE-mNa<sub>x</sub>-T1679A), in which Thr-1679 was replaced with Ala,  
137 was generated from pTRE-mNa<sub>x</sub> [11] using the QuickChange Muta-  
138 genesis kit (Stratagene). Expression plasmids for the N-terminal  
139 FLAG-tagged wild-type Na<sub>x</sub> (pFLAG-mNa<sub>x</sub>) and mutant Na<sub>x</sub>  
140 (pFLAG-mNa<sub>x</sub>-T1679A) were generated by subcloning the respec-  
141 tive cDNAs, into pcDNA-FLAG [14]. The construct for myc-tagged  
142 SAP97 (pMyc-SAP97) was prepared as follows. The full-length  
143 cDNA of mouse SAP97 (GenBank accession number NM\_007862)  
144 was obtained by RT-PCR with mouse brain mRNA, and a myc-epi-  
145 tope tag was attached to the N-terminus of the cDNA using PCR.  
146 Then it was inserted into a mammalian expression vector  
147 pcDNA3.1 (Life Technologies). HEK293T cells (human embryonic  
148 kidney epithelial cells) were maintained in DMEM containing  
149 10% FCS under 5% CO<sub>2</sub> at 37 °C. DNA transfection was performed  
150 by the standard calcium phosphate method.

151 **2.7. Na<sub>x</sub>-expressing C6 cells**

152 The C6M16 cell line, in which mouse Na<sub>x</sub> expression is inducible  
153 under the control of the tetracycline-responsive element (TRE),  
154 was described previously [11]. Cell lines which allow inducible  
155 expression of a PDZ-binding-motif mutant of Na<sub>x</sub> were established  
156 in the same way. Briefly, C6 glioblastoma cells were cotransfected

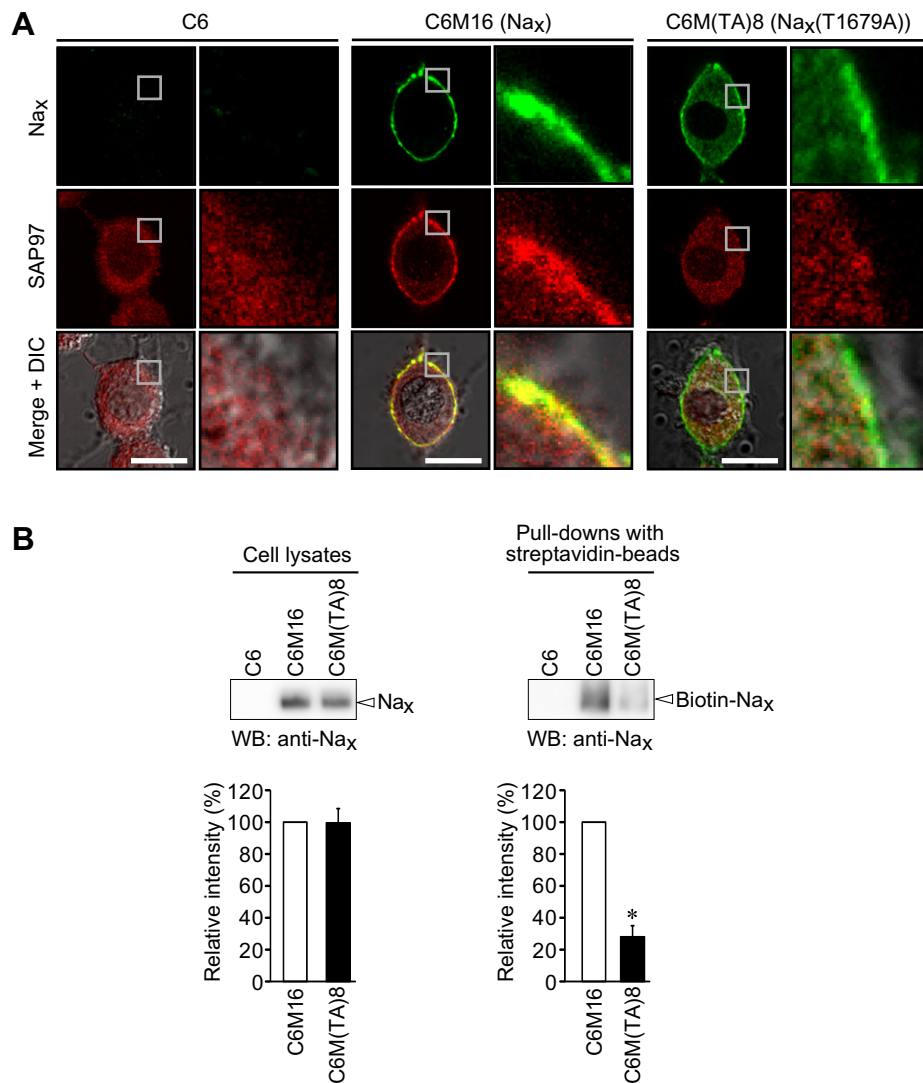


**Fig. 4.** Decrease in cell-surface expression of the Na<sub>x</sub> mutant with Thr-1679 changed to Ala in C6 cells. (A) C6 cells (without expression of Na<sub>x</sub>), C6M16 cells (with expression of wild-type Na<sub>x</sub>) or C6M(TA)8 cells (with expression of mutant Na<sub>x</sub> in the PDZ-binding motif) were fixed, permeabilized, and then stained with anti-Na<sub>x</sub> (green) and anti-SAP97 (red). The fluorescence images merged with differential interference contrast images (DIC) are shown at the bottom. The right images are enlargements of the area enclosed by the square in the left adjacent image, respectively. Scale bars, 10 μm. (B) Western blots of the total cell lysate (left) and biotinylated cell-surface proteins (right) from C6, C6M16, and C6M(TA)8 cells using the anti-Na<sub>x</sub>. Signal intensities were quantified by densitometry and shown as a percentage of the intensity of C6M16. Data are the mean ± SE, *n* = 4 for each; \**P* < 0.01, two-tailed *t* test.

157 with pTRE-mNa<sub>x</sub>-T1679A and pKJ2 carrying the neomycin-resistance  
 158 gene, and then selected with a neomycin-analog G418  
 159 (1.2 mg/ml) in DMEM containing 10% FCS under 5% CO<sub>2</sub> at 37 °C.  
 160 Na<sub>x</sub> expression was induced by the Tet-Off adenoviral vector (Clon-  
 161 tech) in serum-free DMEM containing 1 mM dibutyryl cyclic AMP  
 162 for 36 h. Expression of Na<sub>x</sub> was estimated by Western blotting. A  
 163 clone named C6M(TA)8, which shows the same expression level  
 164 as C6M16 cells, was selected and used for the present study.

## 165 2.8. Co-immunoprecipitation and GST pull-down assays

166 Cells were lysed with a lysis buffer (1% Triton X-100 and  
 167 150 mM NaCl in 10 mM Tris-HCl, pH 7.4) containing protease  
 168 inhibitors (Complete Protease Inhibitor Cocktail, Roche Applied  
 169 Science), and the supernatant was collected by centrifugation. Cell  
 170 extracts obtained were incubated with anti-FLAG M2 antibody  
 171 (Sigma-Aldrich), and the immunocomplexes were precipitated  
 172 using protein G-Sepharose (GE Healthcare). For the GST-pull down  
 173 assay, GST-Na<sub>x</sub>-C-term or GST-Na<sub>x</sub>-C-termΔTQI was first bound to

glutathione-Sepharose beads (GE Healthcare), and the beads were  
 174 incubated with C6 cell extracts. After washing the beads, the bound  
 175 proteins were analyzed by Western blotting.  
 176

## 177 2.9. Biotinylation of cell-surface proteins

178 Cells were washed with 10 mM triethanolamine, pH 7.5 con-  
 179 taining 150 mM NaCl and 2 mM CaCl<sub>2</sub>, and treated with 500 μg/  
 180 ml Sulfo-NHS-Biotin (Pierce) for 30 min on ice. The reaction was  
 181 quenched by washing with a buffer containing 0.1 M glycine, and  
 182 then cells were lysed with the lysis buffer. Na<sub>x</sub> was immunoprecip-  
 183 itated from the cell extracts with anti-Na<sub>x</sub> by using Protein G-  
 184 coated magnetic beads (Dynabeads protein G, Life Technologies),  
 185 and subjected to Western blotting as above.

## 186 2.10. RNA interference

187 Predesigned siRNA against rat SAP97 (siRNA ID, SA-  
 188 SI\_Rn02\_00260207) and its scrambled siRNA were purchased from

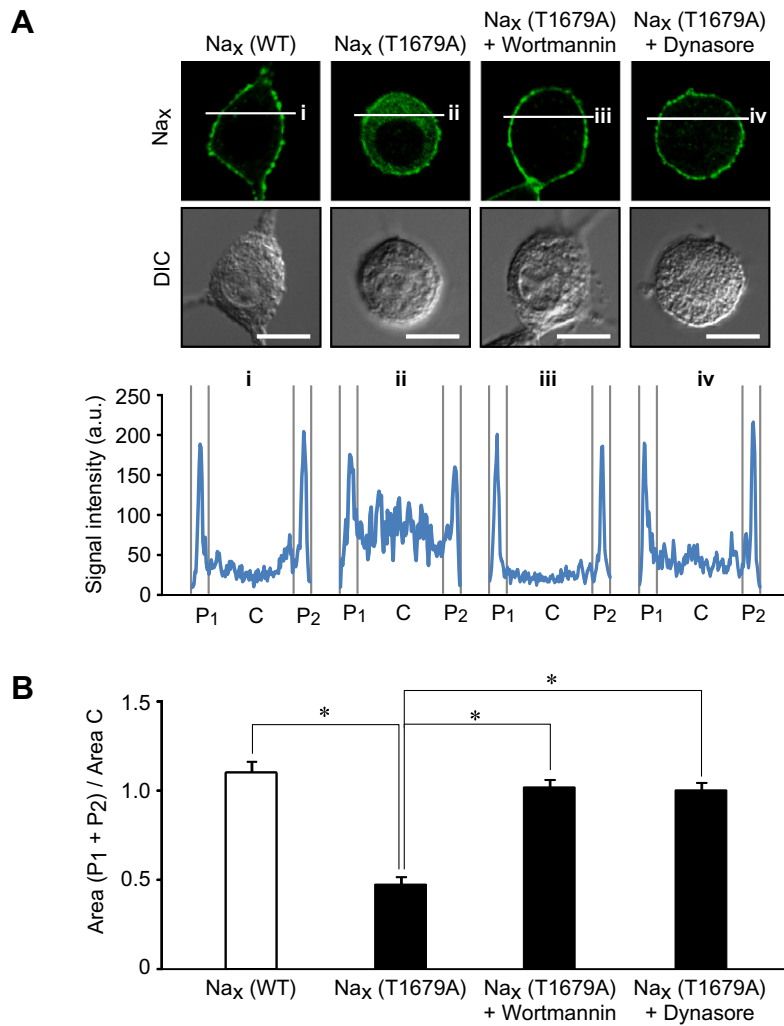


**Fig. 5.** Improvement in surface expression of the Na<sub>x</sub>(T1679A) mutant in C6 cells on treatment with wortmannin and dynasore. (A) Upper panels: Subcellular distribution of the wild-type and T1679A mutant Na<sub>x</sub> in C6 cells. After the induction of Na<sub>x</sub>(T1679A) channels, cells were treated with 100 nM wortmannin or 200 μM dynasore for 6 h. Then the cells were fixed, permeabilized, and stained with anti-Na<sub>x</sub>. Scale bars, 10 μm. Lower graphs: Fluorescence intensity profiles along the white lines in the upper panels. The profile was divided into three parts (P<sub>1</sub>:C:P<sub>2</sub> = 15:70:15 in length). a.u., arbitrary unit. (B) Subcellular distribution of Na<sub>x</sub>. The relative fluorescence intensity of the membrane region to the central region in (A) is presented respectively as the mean ± SE (n = 8 for each); \*P < 0.01, ANOVA followed by Scheffe's test.

189 Sigma–Aldrich. C6 cells (2 × 10<sup>6</sup>) were electroporated with  
190 100 pmol siRNA using the Amaxa Nucleofector (Amaxa) according  
191 to the manufacturer's protocol.

192 **2.11. Intracellular Na<sup>+</sup> imaging**

193 Intracellular Na<sup>+</sup> imaging with sodium-binding benzofuran iso-  
194 phthalate acetoxymethyl ester (SBFI/AM; Molecular Probes) was  
195 performed as described [2].

196 **3. Results**

197 **3.1. Identification of PDZ proteins that interact with Na<sub>x</sub>**

198 We screened for potential interactions between Na<sub>x</sub> and PDZ  
199 proteins using the PDZ-array overlay assay [10,12] with the GST-  
200 fused protein with the C-terminal region of Na<sub>x</sub> (GST-Na<sub>x</sub>-C-term)  
201 (Fig. 1). Proteins spotted on the array are shown in **Supplementary**  
202 **Information (Table. S1)**. Strong positive hits on the first and second  
203 PDZ domains (PDZ1+2) of SAP97, the PDZ domain of CNRasGEF  
204 (also called PDZ-GEF1, RA-GEF-1, or RAPGEF2), and the third PDZ  
205 domain (PDZ3) of LNX1 were identified, along with weaker  
206 positive hits on neuronal nitric oxide synthase (nNOS), Erbb2

207 interacting protein (ERBIN also called LAP2), PDZ3 of zonula  
208 occludens-1 (ZO1, also called Tjp1), GAIP-interacting protein  
209 C-terminus (GIPC, also called synectin or TIP-2), β1-syntrophin,  
210 and DENSIN180 (also called Lrrc7). No binding was detected  
211 with GST-Na<sub>x</sub>-C-term-T1679A (Fig. S1) or control GST (data not  
212 shown), indicating that the native C-terminal PDZ-binding  
213 sequence of Na<sub>x</sub> is essential for the binding with all the potential  
214 partners.

215 **3.2. Coexpression of SAP97 and Na<sub>x</sub> in SFO cells**

216 Among the three strongly positive PDZ proteins, SAP97 was  
217 found to be expressed in the SFO by in situ hybridization  
218 (Fig. 2A), while CNRasGEF and LNX1 were not (data not shown).  
219 Moreover, immunostaining of mouse SFO cells with anti-SAP97  
220 and anti-Na<sub>x</sub> antibodies revealed robust colocalization of the two  
221 proteins at the plasma membrane (Fig. 2B).

222 **3.3. Interaction of Na<sub>x</sub> with SAP97 via its C-terminal PDZ-binding motif**

224 GST-Na<sub>x</sub>-C-term, but not GST-Na<sub>x</sub>-C-termΔTQI (PDZ-binding-  
225 motif deletion mutant), pulled down the native SAP97 from the C6

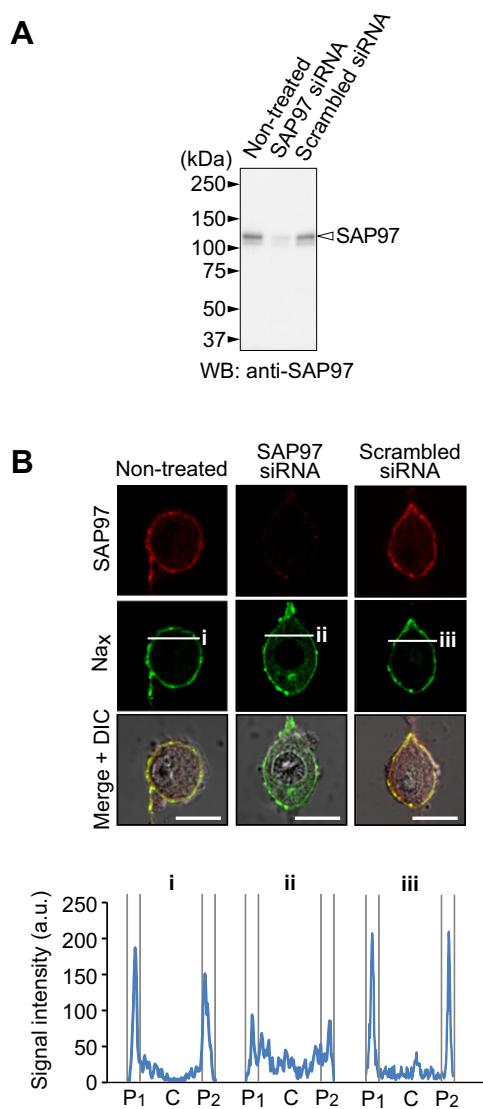


**Fig. 6.** Reduction in the cell-surface expression of Na<sub>x</sub> with depletion of SAP97. (A) Depletion of SAP97 in C6M16 cells. Expression of SAP97 in non-treated C6M16 cells, or C6M16 cells transfected with siRNA for SAP97 or scrambled siRNA was examined by Western blotting. (B) Subcellular distribution of Na<sub>x</sub>. The same cells as above were immunostained with anti-SAP97 and anti-Na<sub>x</sub>. The fluorescence intensity profiles along the white lines are shown below. Scale bars, 10 μm. a.u., arbitrary unit.

cell lysate (Fig. 3A). We next examined the binding of the full-length Na<sub>x</sub> channel and SAP97 in a cellular context. HEK293T cells were transfected with myc-tagged SAP97, together with FLAG-tagged Na<sub>x</sub>, FLAG-tagged Na<sub>x</sub>(T1679A), or a control mock vector (pcDNA-FLAG). When the cell extracts were immunoprecipitated with anti-FLAG antibody, myc-tagged-SAP97 was coimmunoprecipitated with FLAG-tagged Na<sub>x</sub>, but not with the FLAG-tagged T1679A mutant or the control (Fig. 3B). These results verified that Na<sub>x</sub> binds to SAP97 through its C-terminal PDZ-binding motif in cells.

### 3.4. Decreased surface expression of the PDZ-binding-motif mutant of Na<sub>x</sub>

We previously established a C6 glioblastoma cell line, C6M16, in which the expression of Na<sub>x</sub> channels is inducible under the control of the TRE [11]. For the present study, we established another C6 cell line, C6M(TA)8 expressing the Na<sub>x</sub>(T1679A) mutant with a

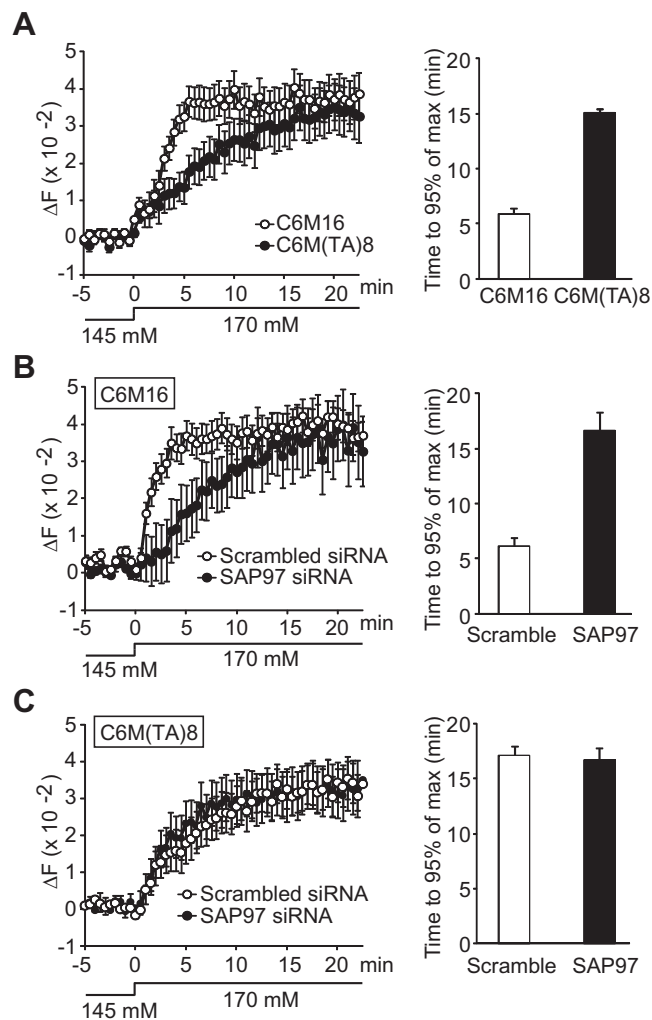


**Fig. 7.** Reduced sodium influx in C6 cells in the absence of any association between Na<sub>x</sub> and SAP97. (A) Left: Na<sup>+</sup> imaging of C6M16 (wild-type Na<sub>x</sub>) and C6M(TA)8 (T1679A mutant Na<sub>x</sub>) cells upon elevation of the extracellular Na<sup>+</sup> concentration from 145 mM to 170 mM. The coordinate gives the fluorescence ratio (ΔF<sub>340/380 nm</sub>) of SBFI, representing the intracellular Na<sup>+</sup> concentration. The physiological 145 mM Na<sup>+</sup> solution was changed to a 170 mM solution at 0 min. Right: Summary of the time to reach 95% of the maximum fluorescence ratio. (B, C) Left: Na<sup>+</sup> imaging of C6M16 (B) or C6M(TA)8 (C) cells expressing siRNA for SAP97 or the control scrambled siRNA. Right: Summary of the time to reach 95% of the maximum fluorescence ratio. Data represent the mean ± SE (n = 40 for each); \*P < 0.01, two-tailed t test.

similar expression level of Na<sub>x</sub> proteins to C6M16 cells, to characterize differences from the wild type.

In the parent C6 cells without expression of Na<sub>x</sub>, SAP97 was detected in the intracellular region (Fig. 4A, left panels). In contrast, in the C6M16 cells with Na<sub>x</sub> expression, SAP97 was clearly observed in the plasma membrane in addition to the cytoplasm (Fig. 4A, middle panels). However, in C6M(TA)8 cells, the signal intensity for Na<sub>x</sub>(T1679A) at the plasma membrane was markedly decreased compared to the wild-type Na<sub>x</sub> and strong signals were detected in the cytoplasm (Fig. 4A, right panels). Indeed, cell-surface biotinylation indicated the surface expression of the mutant Na<sub>x</sub> to be significantly lower than that of the wild-type, while the total amount was equivalent (Fig. 4B). These results suggest that translocation of Na<sub>x</sub> channels to the plasma membrane was impaired, or translocation from the plasma membrane to cytoplasmic area was enhanced, by the loss of function of the PDZ-binding domain. Moreover, the finding that SAP97 is present at the plasma

258 membrane in C6M16 cells, but not in C6M(TA)8 or the parent C6  
259 cells, also indicate that the targeting of SAP97 to the plasma mem-  
260 brane is dependent on the binding with Na<sub>x</sub>.

### 261 3.5. Improvement of the surface expression of the PDZ-binding-motif 262 mutant of Na<sub>x</sub> by inhibition of endocytosis

263 We postulated that SAP97 contributes to the stabilization of Na<sub>x</sub>  
264 at the plasma membrane. If this was the case, inhibitors of endocy-  
265 tosis should increase the surface expression of the T1679A mutant  
266 of Na<sub>x</sub>. Consistent with this idea, incubation with wortmannin, an  
267 inhibitor of endocytosis [15], or dynasore, an inhibitor for dynam-  
268 in-dependent endocytosis [16], markedly ameliorated the surface  
269 expression of the Na<sub>x</sub>(T1679A) mutant (Fig. 5). On the other hand,  
270 the surface expression of wild-type Na<sub>x</sub> was not affected with  
271 these inhibitors (data not shown). These results indicate that bind-  
272 ing with SAP97 via the PDZ-binding motif of Na<sub>x</sub> promotes the sta-  
273 bilization of Na<sub>x</sub> at the plasma membrane.

### 274 3.6. Decrease in the surface expression of Na<sub>x</sub> by reduction of SAP97 275 expression

276 To examine whether the surface expression of Na<sub>x</sub> channels is  
277 stabilized by endogenous SAP97, we electroporated siRNA to  
278 knockdown SAP97 in C6M16 cells. Along with the decrease in  
279 SAP97 expression (Fig. 6A), the surface expression of wild-type  
280 Na<sub>x</sub> was found to be markedly decreased (Fig. 6B).

### 281 3.7. Decrease in Na<sub>x</sub>-mediated sodium influx by PDZ-binding-motif 282 mutation or SAP97 knockdown

283 Finally, we determined the functional relevance of the binding  
284 of Na<sub>x</sub> with SAP97 by performing Na<sup>+</sup>-imaging studies. When the  
285 extracellular Na<sup>+</sup> concentration, [Na<sup>+</sup>]<sub>o</sub> was increased from  
286 145 mM to 170 mM, both C6M16 cells expressing wild-type Na<sub>x</sub>  
287 and C6M(TA)8 cells expressing the Na<sub>x</sub>(T1679A) mutant showed  
288 increases in the intracellular Na<sup>+</sup> concentration, [Na<sup>+</sup>]<sub>i</sub>, and the  
289 level eventually reached the same equilibrium point between Na<sup>+</sup>  
290 influx by Na<sub>x</sub> and Na<sup>+</sup> export by Na<sup>+</sup>/K<sup>+</sup>-ATPase (Fig. 7A). However,  
291 importantly, C6M(TA)8 cells took longer to reach this equilibrium  
292 level than control C6M16 cells. This indicates that the reduction  
293 in the number of surface Na<sub>x</sub> channels diminished the Na<sup>+</sup> influx.

294 Similarly, when SAP97 expression in C6M16 cells was knocked  
295 down with siRNA, the time taken to reach the plateau of [Na<sup>+</sup>]<sub>i</sub> also  
296 increased to approximately the same as that observed in C6M(TA)8  
297 cells (Fig. 7B). Importantly, knockdown of SAP97 in C6M(TA)8 cells  
298 did not slow down the rate of increase in [Na<sup>+</sup>]<sub>i</sub> (Fig. 7C). These  
299 findings clearly indicate that the cell-surface expression of Na<sub>x</sub>  
300 channels is proportional to the increase in [Na<sup>+</sup>]<sub>i</sub> in response to  
301 the increase in [Na<sup>+</sup>]<sub>o</sub>.

## 302 4. Discussion

303 In this study, we found that the PDZ-binding motif at the  
304 C-terminus of Na<sub>x</sub> associates with SAP97 in cells. SAP97 was coex-  
305 pressed with Na<sub>x</sub> in glial cells in the SFO, where Na<sub>x</sub> monitors the  
306 Na<sup>+</sup>-level in body fluids. Disruption of the PDZ-binding motif or  
307 depletion of SAP97 attenuated Na<sub>x</sub>-mediated sodium influx in glial  
308 cells due to the impaired cell-surface expression of Na<sub>x</sub>. SAP97 ap-  
309 pears to ameliorate the cell-surface expression of Na<sub>x</sub> channels by  
310 enhancing protein stability.

311 Among voltage-gated sodium channels, Na<sub>v</sub>1.5 has also been re-  
312 ported to interact with SAP97 via its C-terminal PDZ-binding motif,  
313 and the amount of Na<sub>v</sub>1.5 on the cell surface is decreased in SAP97-  
314 silenced myocytes, although the mechanism remains unclear [17].

SAP97 is a member of the membrane-associated guanylate kinase  
(MAGUK) family along with PSD-95, PSD-93, and SAP102. MAGUK  
family members are known to regulate the function, localization,  
and trafficking of ion channels and receptors [8,18–20]. We found  
that both the mutation of the PDZ-binding motif and depletion of  
SAP97 attenuated the sodium influx in response to the increase  
of [Na<sup>+</sup>]<sub>o</sub>, due to the decrease in the amount of Na<sub>x</sub> at the cell sur-  
face (Fig. 4). Thus SAP97 appears to be an important component for  
the [Na<sup>+</sup>]<sub>o</sub>-sensing mechanism in the SFO, which is involved in reg-  
ulation of the surface expression of the sensor channel.

We also identified a number of candidate proteins other than  
SAP97, which may interact with Na<sub>x</sub> (Fig. 1C). CNRasGEF is a guan-  
ine nucleotide exchange factor responsible for sustained activation  
of the Rap1/2 small GTPase [21]. LNX1, an E3 ubiquitin-protein li-  
gase, is expressed in the non-myelinating perisynaptic Schwann  
cells in adult mice [22]. Although these molecules were not de-  
tected in the SFO, further study is required to make clear whether  
these proteins interact with Na<sub>x</sub> in other Na<sub>x</sub>-positive cell types,  
such as non-myelinating Schwann cells, dorsal root ganglion neu-  
rons, and Alveolar type II cells [23].

## Acknowledgments

We thank Norie Nakanishi and Seiko Miura for technical assis-  
tance and Akiko Kodama for secretarial assistance. This work was  
supported by Grants-in-Aid from the Ministry of Education, Cul-  
ture, Sports, Science, and Technology (MEXT) of Japan.

## Appendix A. Supplementary data

Supplementary data associated with this article can be found, in  
the online version, at <http://dx.doi.org/10.1016/j.febslet.2012.09.018>.

## References

- Andersson, B. (1977) Regulation of body fluids. *Annu. Rev. Physiol.* 39, 185–200.
- Hiyama, T.Y., Watanabe, E., Ono, K., Inenaga, K., Tamkun, M.M., Yoshida, S. and Noda, M. (2002) Na<sub>x</sub> channel involved in CNS sodium-level sensing. *Nat. Neurosci.* 5, 511–512.
- Noda, M. and Hiyama, T.Y. (2005) Sodium-level-sensitive sodium channel and salt-intake behavior. *Chem. Senses* 30, i44–i45. Suppl 1.
- Noda, M. (2007) Hydromineral neuroendocrinology: mechanism of sensing sodium levels in the mammalian brain. *Exp. Physiol.* 92, 513–522.
- Watanabe, E., Hiyama, T.Y., Shimizu, H., Kodama, R., Hayashi, N., Miyata, S., Yanagawa, Y., Obata, K. and Noda, M. (2006) Sodium-level-sensitive sodium channel Na<sub>x</sub> is expressed in glial laminae processes in the sensory circumventricular organs. *Am. J. Physiol. Regul. Integr. Comp. Physiol.* 290, 568–576.
- Watanabe, E., Fujikawa, A., Matsunaga, H., Yasoshima, Y., Sako, N., Yamamoto, T., Saegusa, C. and Noda, M. (2000) Na<sub>2</sub>/NaG channel is involved in control of salt-intake behavior in the CNS. *J. Neurosci.* 20, 7743–7751.
- Hiyama, T.Y., Watanabe, E., Okado, H. and Noda, M. (2004) The subfornical organ is the primary locus of sodium-level sensing by Na<sub>x</sub> sodium channels for the control of salt-intake behavior. *J. Neurosci.* 24, 9276–9281.
- Kim, E. and Sheng, M. (2004) PDZ domain proteins of synapses. *Nat. Rev. Neurosci.* 5, 771–781.
- Giallourakis, C., Cao, Z., Green, T., Wachtel, H., Xie, X., Lopez-Illasaca, M., Daly, M., Rioux, J. and Xavier, R. (2006) A molecular-properties-based approach to understanding PDZ domain proteins and PDZ ligands. *Genome Res.* 16, 1056–1072.
- He, J., Bellini, M., Inuzuka, H., Xu, J., Xiong, Y., Yang, X., Castleberry, A.M. and Hall, R.A. (2006) Proteomic analysis of β-adrenergic receptor interactions with PDZ scaffold proteins. *J. Biol. Chem.* 281, 2820–2827.
- Shimizu, H., Watanabe, E., Hiyama, T.Y., Nagakura, A., Fujikawa, A., Okado, H., Yanagawa, Y., Obata, K. and Noda, M. (2007) Glial Na<sub>x</sub> channels control lactate signaling to neurons for brain [Na<sup>+</sup>] sensing. *Neuron* 54, 59–72.
- Fam, S.R., Paquet, M., Castleberry, A.M., Oller, H., Lee, C.J., Traynelis, S.F., Smith, Y., Yun, C.C. and Hall, R.A. (2005) P2Y<sub>1</sub> receptor signaling is controlled by interaction with the PDZ scaffold NHERF-2. *Proc. Natl. Acad. Sci. USA* 102, 8042–8047.
- Suzuki, R., Shintani, T., Sakuta, H., Kato, A., Ohkawara, T., Osumi, N. and Noda, M. (2000) Identification of RALDH-3, a novel retinaldehyde dehydrogenase, expressed in the ventral region of the retina. *Mech. Dev.* 98, 37–50.

- 384 [14] Fukada, M., Kawachi, H., Fujikawa, A. and Noda, M. (2005) Yeast substrate- 400  
385 trapping system for isolating substrates of protein tyrosine phosphatases: 401  
386 isolation of substrates for protein tyrosine phosphatase receptor type z. 402  
387 Methods 35, 54–63. 403
- 388 [15] Gong, Q., Weide, M., Huntsman, C., Xu, Z., Jan, L.Y. and Ma, D. (2007) 404  
389 Identification and characterization of a new class of trafficking motifs for 405  
390 controlling clathrin-independent internalization and recycling. J. Biol. Chem. 406  
391 282, 13087–13097. 407
- 392 [16] Kirchhausen, T., Macia, E. and Pelish, H.E. (2008) Use of dynasore, the small 408  
393 molecule inhibitor of dynamin, in the regulation of endocytosis. Methods 409  
394 Enzymol. 438, 77–93. 410
- 395 [17] Petitprez, S., Zmoos, A.F., Ogrodnik, J., Balse, E., Raad, N., El-Haou, S., Albesa, M., 411  
396 Bittihn, P., Luther, S., Lehnart, S.E., Hatem, S.N., Coulombe, A. and Abriel, H. 412  
397 (2011) SAP97 and dystrophin macromolecular complexes determine two 413  
398 pools of cardiac sodium channels  $Na_v1.5$  in cardiomyocytes. Circ. Res. 108, 414  
399 294–304. 415
- [18] Zheng, C.Y., Seabold, G.K., Horak, M. and Petralia, R.S. (2011) MAGUKs, 400  
synaptic development, and synaptic plasticity. Neuroscientist 17, 493–512. 401
- [19] Elias, G.M. and Nicoll, R.A. (2007) Synaptic trafficking of glutamate receptors 402  
by MAGUK scaffolding proteins. Trends Cell Biol. 17, 343–352. 403
- [20] Hidalgo, P. and Neely, A. (2007) Multiplicity of protein interactions and 404  
functions of the voltage-gated calcium channel  $\beta$ -subunit. Cell Calcium 42, 405  
389–396. 406
- [21] de Rooij, J., Boenink, N.M., van Triest, M., Cool, R.H., Wittinghofer, A. and Bos, 407  
J.L. (1999) PDZ-GEF1, a guanine nucleotide exchange factor specific for Rap1 408  
and Rap2. J. Biol. Chem. 274, 38125–38130. 409
- [22] Young, P., Nie, J., Wang, X., McGlade, C.J., Rich, M.M. and Feng, G. (2005) LNX1 410  
is a perisynaptic Schwann cell specific E3 ubiquitin ligase that interacts with 411  
ErbB2. Mol. Cell. Neurosci. 30, 238–248. 412
- [23] Watanabe, E., Hiyama, T.Y., Kodama, R. and Noda, M. (2002)  $Na_x$  sodium 413  
channel is expressed in non-myelinating Schwann cells and alveolar type II 414  
cells in mice. Neurosci. Lett. 330, 109–113. 415